First-Principles Theoretical Study of Molecular HCl Adsorption on a Hexagonal Ice (0001) Surface

Yves A. Mantz, Franz M. Geiger, Luisa T. Molina, and Mario J. Molina

Department of Earth, Atmospheric, and Planetary Sciences and of Chemistry, Massachusetts Institute of Technology, Cambridge, Massachusetts 02139

Bernhardt L. Trout*

Department of Chemical Engineering, Massachusetts Institute of Technology, Cambridge, Massachusetts 02139

Received: March 1, 2001; In Final Form: May 15, 2001

A key step in the mechanism of polar ozone depletion involves the interaction of HCl with the particles that constitute polar stratospheric clouds. These particles exist as hexagonal ice I*h* crystals below approximately 185 K. As a first step, we examine the binding of molecular HCl to a number of extended surface models of the basal (0001) face of hexagonal ice in addition to a cluster model representative of an unreconstructed adsorption site. Calculations are performed using gradient-corrected density-functional theory and high-order correlation methods. After correcting for zero-point energies, we estimate the molecular binding energy and enthalpy at 185 K to be 23 and 25 kJ/mol, respectively, for low (single-molecule) HCl coverage. These estimates decrease by a few kJ/mol at higher HCl coverage and are based partially on a low density of dangling surface OH groups. Our results set the stage for future studies addressing the possible ionization of molecularly adsorbed HCl using first-principles molecular dynamics.

I. Introduction

It is now widely accepted that the annual formation of the Antarctic ozone hole during early polar spring is a direct result of the heterogeneous reaction of stable forms of chlorine on polar stratospheric clouds (PSCs) between 14 and 19 km altitude.[1] A very important example is Rx. (1) depicting production of active chlorine and sequestration of NO_x on Type II PSCs (hexagonal ice I*h* crystals), which form at a few degrees below the frost point of ice,[2,3] which is 188 K for a typical water vapor pressure of 2.0×10^{-4} Torr.[4,5] The photolysis of $Cl_2(g)$ ultimately leads to the gas-phase catalytic destruction of ozone, while sequestration of NO_x prevents re-formation of relatively stable $ClONO_2(g)$.[6]

$$HCl(ads) + ClONO_2(g) \xrightarrow{ice} Cl_2(g) + HNO_3(ads) \quad (1)$$

Although studied experimentally,[7−9] the mechanism of Rx. (1) (and other, related reactions) is still not known. The reaction of HCl with $ClONO_2$ on the surface of ice is known to proceed rapidly,[10] in contrast to the prohibitively slow gas-phase reaction;[11] this suggests an ionic-type mechanism may be operative in the presence of ice. As reviewed elsewhere,[12,13] a partially disordered transition region is present on the surface of ice at temperatures below the bulk freezing point. This "quasi-liquid layer," as it is sometimes referred to in the literature, may facilitate ionic dissociation of HCl, a mechanism originally proposed by our laboratory.[14] Another possibility is that HCl is incorporated into the ice lattice at the surface,[15,16] which is known from experiments to be very dynamic: If the ice surface is in equilibrium with its vapor phase, ∼10−100 bilayers per second are adsorbed and desorbed at 185 K.[17] Subsequent reaction of HCl with $ClONO_2$ involves proton transfer in the ice lattice accompanied by nucleophilic attack of Cl^- on the $Cl^{\delta+}$ in $ClONO_2$.[18,19] A third possibility involves several associative and dissociative steps catalyzed by NO_3^-.[20]

A key first step involved in the mechanism of Rx. (1) is the uptake of HCl.[21] Using smooth and/or well-characterized ice films, experimentalists have shown the uptake of HCl is $\sim 10^{13}-10^{14}$ molecule/cm^2 at stratospherically relevant temperatures and HCl partial pressures.[7,22,23] Direct observation of HCl at ice surfaces remains difficult due to the technical challenges of performing experiments with molecular specificity under conditions typical of the polar stratosphere ($\sim 10^{-4}$ Torr water vapor), where traditional surface-science techniques, which require ultrahigh vacuum conditions, are often not feasible. Thus, it is not known whether HCl exists in an ionic or molecular form at (or near) the ice surface. Spectroscopic,[24−26] and other,[27] evidence indicates an ionic form of HCl at low temperatures (less than 180 K) and partial pressures where ionic hydrates of HCl are known to be thermodynamically stable. However, on the basis of the HCl−ice phase diagram,[28,29] bulk hydrates of HCl are not thought to exist in the polar stratosphere. In addition, other experimentalists have inferred a molecularly adsorbed form.[30−35]

Several of the experimental studies that suggest a molecular form give an estimate of the energy of interaction, but many assumptions are necessary in order to obtain values. Furthermore, these experiments are not generally performed under both temperature and equilibrium conditions with respect to water vapor applicable to the polar stratosphere. In a recent molecular beam study,[31] a lower limit of 31−38 kJ/mol to the binding energy at 165 K of HCl on slowly condensing ice with less than 5×10^{12} molecule HCl/cm^2 adsorbed was found. An upper limit of 25 kJ/mol for HCl interacting with slowly evaporating HCl-covered ice was also determined assuming a frequency

* Corresponding author. E-mail: trout@mit.edu. Fax: 617-258-8224.

10.1021/jp010817u CCC: $20.00
Published on Web 06/22/2001

factor of 10^{13} s^{-1}, suggesting a coverage dependence of 10 kJ/mol. In two other experimental studies, the activation energy for desorption was estimated. In the first study,[32] molecular beams of HCl were reflected from amorphous and crystalline ice surfaces held at 100−126 K and were detected using mass spectroscopy, and a model was developed to obtain activation energies for HCl desorption of 28 ± 2 and 26 kJ/mol, respectively. In the second study,[33] adopting a value of 10^{13} s^{-1} for the frequency factor, a value of 33 ± 5 kJ/mol assumed to be independent of the total surface coverage of HCl was estimated at 140 K from temperature-programmed desorption. Last, an HCl binding enthalpy of 46 kJ/mol at 200 K was estimated by Elliott et al.,[34] who analyzed an experimental isotherm reported by Hanson and Mauersberger[29] and then assumed that the change in entropy was the same as that for liquefaction of pure HCl(g). For reference, note the limiting enthalpy of solution of HCl, which describes $HCl(g) \rightarrow H^+(aq) + Cl^-(aq)$ at 298 K and includes ionization of HCl and hydration of infinitely separated product ions, is 75 kJ/mol.[36,37] This summary indicates that there is currently uncertainty in the measured value of the energy of adsorption, providing another motivation to study the interaction of HCl with ice theoretically.

As a first step, theorists have studied the interaction of molecular HCl with model ice surfaces. Small cluster models have been (by necessity) used in high-level ab initio studies.[38−42] Other studies with periodic surfaces, which are a more realistic model of an unreconstructed hexagonal ice surface, have either been performed with a limited basis set at the Hartree−Fock level of theory, requiring an indirect estimate of correlation effects,[43] or have relied on an adjustable potential parameterized for the study of liquid water at STP rather than hexagonal ice.[44−47] In recent years, using cluster[38,48,49] as well as extended surface models,[15,16,50,51] several theoretical studies have focused on the role that water molecules play in the ionization of HCl, but these studies also suffer from one (or more) of the above limitations.

In this article, we lay the groundwork for investigating, using first-principles molecular dynamics, the atmospheric fate and the possible ionization of HCl on ice. We perform geometry optimizations of molecular HCl on cluster and well as extended ice surface models, thereby allowing comparison of different models in a careful, consistent manner. Binding energies incorporating zero-point energies are also calculated. Our method treats exchange and correlation effects explicitly and employs large basis sets, thereby providing a test of the validity of, and serving as an important complement to, previous theoretical approaches. In this study, both the surface coverage of HCl and the number of dangling (non-hydrogen-bonding) OH groups are varied. To our knowledge, there are no previous theoretical studies of varying HCl surface coverage, and there is only one recent quantum-classical study investigating the role of varying number of OH groups on the ionization of HCl.[52]

The organization of this paper is as follows. Our models and our system of nomenclature are described in section II. Our approach is described in section III. The main results are presented in section IV. A correction estimate for our use of the BLYP functional and pseudopotentials/plane waves is developed in section IV A, while correction estimates to the binding energy and enthalpy incorporating zero-point energies and thermal effects are made in section IV B. Results for molecular HCl adsorption on extended ice surface models incorporating these corrections are then given in section IV C. The results on extended surfaces are discussed further, and a best estimate of the binding energy and enthalpy at finite temperatures is developed, in section V. Atmospheric implications are briefly discussed in section VI. Concluding remarks are made in section VII.

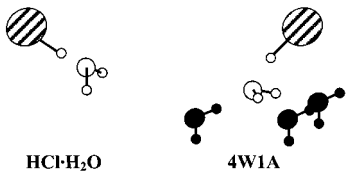

Figure 1. Depiction of HCl•H_2O and the cluster 4W1A.

II. Ice Surface Models

As a first attempt to model adsorption of molecular HCl on a hexagonal ice basal (0001) face,[53] which may be the most prevalent under polar stratospheric conditions,[16] the interaction of molecular HCl with a single water molecule as well as with a small cluster model representative of an adsorption site was studied. These models are depicted in Figure 1. Each model was placed in a large cubic simulation cell with $a = 10$ Å to prevent interaction with periodic images.[54] The cluster model is named 4W1A in order to distinguish it from the cyclic structure HCl•$(H_2O)_4$,[40] which corresponds to the global minimum for HCl interacting with four water molecules.

Infinite surface or slab models were developed for comparison to simple cluster models. This development follows our earlier study of an ice slab.[13] Because the density of dangling OH groups on ice is not known experimentally, models with different numbers of dangling OH groups were developed. Other considerations included having each model satisfy the Bernal−Fowler ice rules,[55] where each oxygen atom is given two OH bonds and two hydrogen bonds arranged tetrahedrally; having a full-bilayer termination, where each surface water molecule forms three hydrogen bonds, which is more stable by 58 kJ/mol (per simulation cell) at the Hartree−Fock level than a half-bilayer termination, where each surface water molecule forms only one hydrogen bond;[56] and, last, having a net dipole moment as small as possible, because real ice is known to possess a zero net dipole moment due to proton disorder.[57]

Our extended surface models with the maximum possible number of HCl adsorbates are shown in Figure 2. To differentiate the models on the basis of the total number x of water molecules, the number y and position p of HCl adsorbates, the number z of dangling OH groups, and whether the bottom bilayer is fixed f to its optimized bulk position, a straightforward nomenclature xWyA$^p z$H(f) is adopted. To illustrate, 16W1A2Hf specifies a model with **16 W**ater molecules, **1** HCl **A**dsorbate bonded to oxygen atom O1, **2** dangling O**H** groups, and a **f**ixed bottom bilayer. If the site O2 (or O3) is occupied instead of O1, this is explicitly indicated, e.g., 16W1A^{O2}2Hf. If no HCl molecules are adsorbed to the slab, yA is omitted, e.g., 16W2Hf. As the final example, the name of a model with **32 W**ater molecules, **2** HCl **A**dsorbates bonded to oxygen atoms O1 and O2, **2** dangling O**H** groups, and no fixed bottom bilayer is 32W2A2H.

For our slab models, the oxygen atoms were placed such that a hexagonal ice super cell with full-bilayer termination was formed with dimensions $2a = 9.046$ Å and $c = 7.367$ Å, where the lattice constants $a = 4.523$ Å and $c = 7.367$ Å are, from experiment, those of hexagonal ice at 273 K.[58] For models with eight layers and 32 water molecules, the dimensions are $2a = 9.046$ Å and $2c = 14.734$ Å. A total number of (bare oxygen) adsorption sites of three, two, or one are available for models with one, two, or three dangling OH groups, respectively, giving

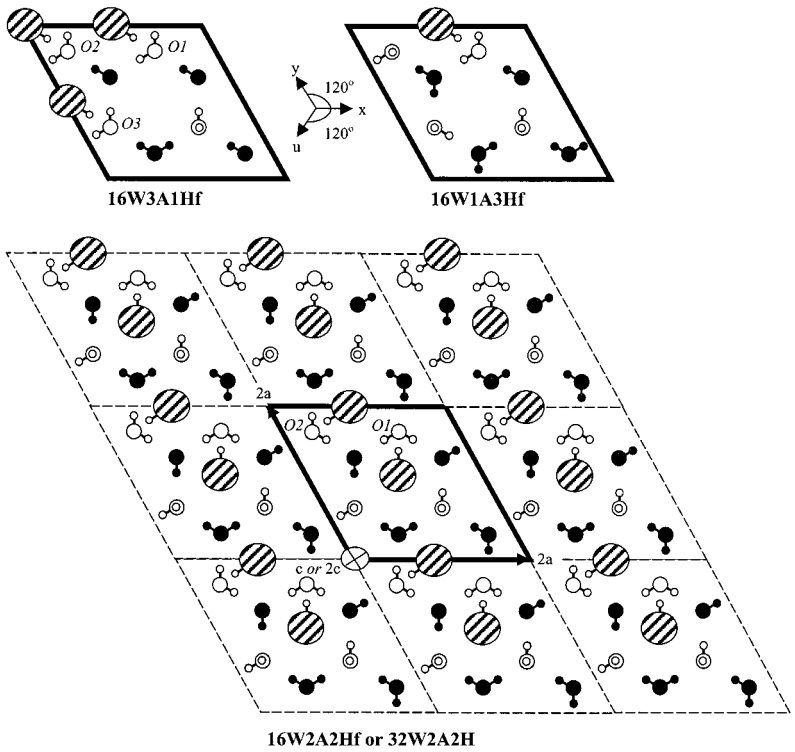

Figure 2. The (0001) face depicted for 16W3A1Hf, 16W2A2Hf, 32W2A2H, and 16W1A3Hf. The simulation cell is outlined in thick black. White atoms are in the top (first) layer, while black atoms are in the underlying (second) layer; for clarity, only atoms in the top (first) bilayer are shown. As a reminder that periodic boundary conditions were used in all directions, a 3×3 periodic representation of 16W2A2Hf (or 32W2A2H) is shown. The naming of these models is explained in the text. Models with either 16 or 32 water molecules have either four or eight layers, respectively, of four water molecules each. The adsorption sites O1, O2, and O3 are labeled if there is more than one possible adsorption site.

a maximum possible surface coverage of 4.2×10^{14} molecule/cm^2 equal to three divided by the rhombus area.

To create a slab model with a specified number of dangling OH groups, all possible arrangements of the hydrogen atoms that satisfied the Bernal-Fowler ice rules were generated systematically with a computer program written in our laboratory (see Supporting Information), and from all of these allowed models, the model with the smallest net dipole moment was selected. Other methods[59,60] have been developed to create models of bulk ice with a zero net dipole moment; our method, however, is readily applied to slab models because it takes into account a (surface) termination of the hydrogen-bond network. The net dipole moment of each slab model was calculated using two methods. First, we assumed that each water molecule had a dipole moment of 3.09 D,[61,62] and that the dipole vector went from the oxygen atom through the molecule's center-of-mass, which gave the same results as the center-of-charge assuming $+\delta$ on each hydrogen atom and -2δ on each oxygen atom. In addition, each HCl molecule was given a dipole moment of 1.11 D.[39] For the second method, Berry-phase calculations were performed,[63] with corrections according to King-Smith and Vanderbilt.[64] These first-principles calculations were performed with a plane-wave basis set and periodic boundary conditions applied as described in section III.

The net dipole moment for the optimized ice slabs 16W2Hf and 32W2H, each with two dangling OH groups, is between 0.01 and 0.1 D assuming fixed dipole values and is only slightly larger, 0.2 and 1.6 D, respectively, when calculated from first principles. The net dipole moment for the optimized ice slab 16W1Hf is 13.1 D assuming fixed values and 8.1 D from first principles, while that for 16W3Hf is 12.2 and 7.2 D assuming fixed values and from first principles, respectively. The projection of the net dipole moment in the *x*,*y*-plane is less than 1 D for these models. The net dipole moments for slab models with HCl adsorbed are given in section IV C. The large net dipole moments of 16W1Hf and 16W3Hf are a consequence of the top (surface) bilayer and (because of the ice rules) each underlying bilayer having an unequal number of dangling OH groups pointing "up" vs "down" into the bulk. In section V, we discuss the consequences of the large net dipole moments and show that they do not lead to a large variation in the binding energy of HCl.

A three-dimensional perspective of one slab model interacting with two HCl molecules is shown in Figure 3. The *c*-dimension of the simulation cell is 8 Å + c = 15.367 Å (or 8 Å + 2c = 22.734 Å for slabs with 32 water molecules), where a consistent-sized surface vacuum region of 8 Å was added in order to mimic an isolated slab. To select an appropriate-sized vacuum region, the vacuum region of the model with the largest dipole moment (16W2A1Hf) was systematically increased and the model re-optimized until the change in atomic positions was negligible, of the order of a few thousandths of one angstrom (for atoms involved in binding, and less for other atoms), as was the change in binding energy of molecular HCl, less than 1 kJ/mol.

In section IV C we present results that show that four layers, with the bottom two fixed, are adequate for modeling adsorption. For a model with four layers, the lateral cell dimensions are as large as computationally practical.

III. Methodology

Density-functional theory[65,66] using a plane-wave basis set[67−69] was used to describe the electronic state of our system. The BLYP functional[70,71] was used for the exchange and correlation energies of the system, and Troullier−Martins pseudopotentials[72,73] were used to describe the core and valence

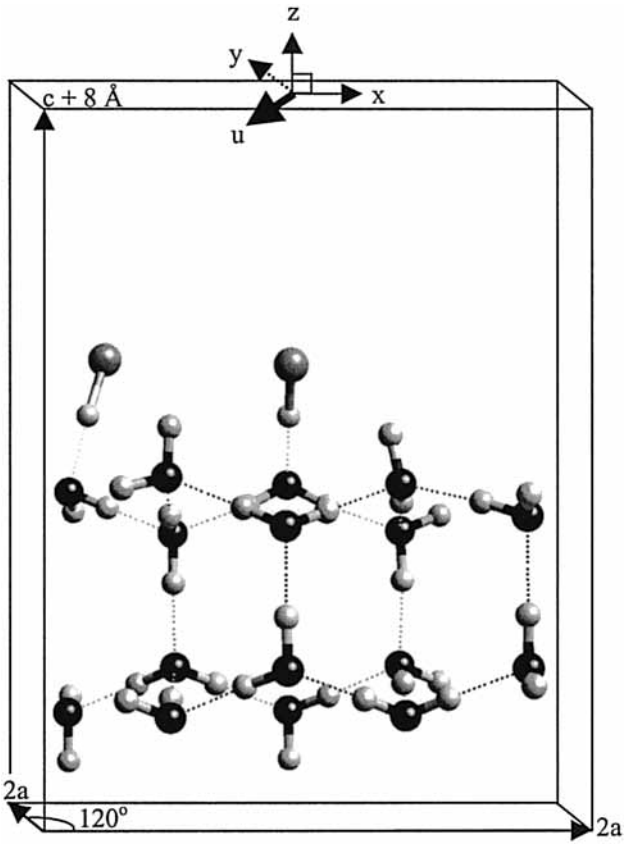

Figure 3. The $(0\bar{1}10)$ face, one of six prism faces perpendicular to (0001), of the optimized slab model 16W2A2Hf. The simulation cell, with the surface vacuum region of 8 Å, is superimposed.

atomic regions. This functional and pseudopotentials were found previously to describe both liquid water[54] and hexagonal ice[13] accurately. CPMD version 3.0f was used for all geometry optimizations except for those with constrained dihedral angles, for which CPMD version 3.3f was used.[74] Periodic boundary conditions were used in all directions. To facilitate convergence, initial geometries similar to previously published structures were used for HCl•H_2O, 4W, and 4W1A.[39,41] Optimized bulk ice[13] was the starting point for the slabs. Other studies[44,52] have shown that HCl binds preferentially with its hydrogen to a surface water oxygen atom. The geometry reported for 4W1A at the MP2 level of theory with a 6-311++G(d,p) basis set was used for initial placement of the HCl adsorbate(s).[39] The bottom bilayer of our slab models was held fixed in order to mimic an infinite bulk, and in section IV C, it is shown that the interaction of HCl is not affected.

Two different methods were used to optimize the geometry. The first method, DIIS with three vectors combined with a quasi-Newton method (using BFGS) for optimization of the ionic positions,[75,76] was used to optimize HCl, H_2O, HCl•H_2O, and the test molecules Cl_2, ClO, HOCl, and $ClONO_2$. The second method, based on simulated annealing,[77] was used to optimize 4W and 4W1A with constrained dihedral angles, as well as the slab models. For both methods, a basis-set cutoff of 70.0 Rydbergs was used; for the second method, a scaling factor of 0.9 for the velocities was used in addition to a fictitious mass of 1100.0 au for the electrons and a time step of 7.0 au (0.17 fs) for the integrator. For the slab models, convergence was slow due to a shallow potential surface and a large number of hydrogen-bonding interactions. Optimizations performed with either method are labeled "BLYP/plane waves" in subsequent tables.

Before performing any geometry optimizations with HCl, an important first step was the development of a pseudopotential for chlorine. To test our method with different chlorine pseudopotentials, geometries for HCl and other small, stratospherically relevant molecules containing chlorine atoms were optimized, including Cl_2, ClO, HOCl, and $ClONO_2$. Our choice of pseudopotential and functional overestimates slightly most bond lengths, and Cl−O and Cl−Cl bonds by less than 0.1 Å. In Table 1, results for HCl are summarized, along with previously published theoretical results[40,41] and the experimental bond length.[78] The density-functional methods seem to overestimate the HCl bond length by a few hundredths of one Ångstrom. Our equilibrium dissociation energy D_e of 421 kJ/mol for HCl underestimates the experimental value of 445.5 kJ/mol calculated from the spectroscopic dissociation energy D_o and anharmonicity constants ω_e and $\omega_e\chi_e$ using $D_e \approx D_o + {}^1/_2\omega_e - {}^1/_4\omega_e\chi_e$.[78] In this study, because elongation of HCl is not substantial and dissociation does not occur, it is reasonable to assume that our systematic underestimation of the HCl bond energy of 25 kJ/mol will not significantly affect binding energy calculations. Our results and those of Packer and Clary for H_2O are also given in Table 1. Our results using plane waves are identical to those previously obtained.[54] The results for H_2O are accurate to within 0.01−0.02 Å and 1−2°.[79]

Use of the BLYP functional and pseudopotentials in a plane-wave calculation is known to underestimate the hydrogen-bond energy for the water dimer by 4 kJ/mol (18%), the smallest error of the variety of functionals used.[54] To estimate the error for the various hydrogen bonds in our study, HCl•H_2O and its constituent molecules were optimized using Gaussian 94,[80] fixing symmetries and the hydrogen-bond angle to ∠HOCl = 180° for HCl•H_2O. Optimizations were performed at the MP2 level of theory[81,82] with the 6-311++G(d,p) basis set;[83−88] at the MP2 and BLYP levels of theory with larger basis sets, cc-pVTZ and cc-pVQZ;[89−91] and at a higher level of theory, QCISD(T),[92] with the 6-311++G(d,p) basis set; these method/basis-set combinations are labeled in Table 1 as MP2/6-311++G(d,p), BLYP/cc-pVTZ, and so on.

For comparison to results obtained experimentally on bulk ice, optimizations of HCl, 4W, and 4W1A were performed in Gaussian 94 using density-functional theory with a BLYP functional and a 6-311++G(d,p) basis set. Zero-point energies were calculated as well as thermal corrections from harmonic frequencies generated using a frequency scaling factor[93,94] of 0.9940 in order to obtain energies and enthalpies at 165, 185, and 200 K, where 165 and 200 K were chosen to compare with experiment.

IV. Optimized Geometries and Binding Energies

A. HCl•H_2O. The calculated geometry and binding energy of HCl•H_2O is given in Table 1 using different methods and basis sets, and these results are compared with previously published theoretical[40,41] and experimental[95] data. The different theoretical approaches are in reasonable agreement: Upon forming the complex, HCl elongates slightly, while the geometry of H_2O in the complex is not significantly different from that of the isolated molecule. Ideally, we would like to be able to compare the binding energies in Table 1 to an experimental value. An alternative is comparison with a high-level theoretical result, which is estimated below and presented in Table 1 as "basis set, correlation corrected."

We first make an estimate of the binding energy in the infinite basis set limit at the MP2 level of theory. From Table 1, the uncorrected binding energies at the MP2 level of theory with a

TABLE 1: Optimized Geometry of H_2O, HCl, and HCl•H_2O and Binding Energy of HCl•H_2O Uncorrected ($-\Delta E_e^N$) and Corrected ($-\Delta E_e^B$) for Basis Set Superposition Error Using the Function Counterpoise Method

	isolated molecules			isolated HCl•H_2O							
		H_2O									
method/basis set	HCl (Å)	OH (Å)	∠HOH (deg)	HCl (Å)	O···H (Å)	∠OHCl (deg)	OCl (Å)	OH (Å)	∠HOH (deg)	$-\Delta E_e^N$ (kJ/mol)	$-\Delta E_e^B$ (kJ/mol)
BLYP/plane waves[a]	1.304	0.973	104.4	1.332	1.842	179.5	3.174	0.973	105.2		23
B3LYP/D95++(p,d)[b]	1.289			1.313	1.820	177.6		0.968		28	19
MP2/6-31G(2dp)[c]	1.271	0.961	104.8	1.287	1.910		3.196	0.962	105.2		22
MP2/6-311++G(d,p)	1.273	0.960	103.4	1.287	1.902	180	3.189	0.961	104.3	27	20
MP2/cc-pVTZ	1.273	0.959	103.5	1.293	1.849	180	3.141	0.961	104.4	29	22
MP2/cc-pVQZ	1.273	0.958	104.0	1.292	1.852	180	3.145	0.959	104.8	26	23
QCISD(T)/6-311++G(d,p)	1.278	0.960	103.4	1.288	1.935	180	3.223	0.961	104.2	26	18
BLYP/cc-pVTZ	1.293	0.972	103.8	1.322	1.831	180	3.152	0.973	104.7	29	22
BLYP/cc-pVQZ	1.292	0.970	104.2	1.319	1.849	180	3.168	0.972	104.9	25	21
basis set, correlation corrected											23
experiment	1.27455[d]	0.9572[e]	104.52[e]			180.0[f]	3.2151[f]				

[a] For methods using (nonlocal) plane waves, basis set superposition error is zero. [b] Reference 40. [c] Reference 41. [d] Reference 78. [e] Reference 79. [f] Reference 95. Structure of $^{35}ClH\cdots OH_2$ was obtained from analysis of microwave data.

TABLE 2: Interaction of HCl with Isolated Cluster Model 4W[a]

method/basis set	HCl (Å)	OH (Å)	∠OHCl (deg)	Cl···H′ (Å)	$-\Delta E_e^N$ (kJ/mol)	$-\Delta E_e^B$ (kJ/mol)	$-\Delta E_o^B$ (kJ/mol)
BLYP/plane waves[b]	1.354	1.761	164.1			27	
BLYP/6-311++G(d,p)	1.339	1.768	169.5		33	30	21
MP2/6-311++G(d,p)[c]	1.296	1.894	155.9		34	26	
MP2/6-31G(2dp)[d]	1.303, 1.323	1.787, 1.657				32, 30	21, 18
MP2/6-31G(d,p)[e,f]	1.294	1.835		2.974, ∼3		38	
corr. HF/6-31G(d)[e,g]	1.28	1.95		3.15, 3.85	46	40	32

[a] Unless otherwise noted. Column headings are as follows: Optimized geometry, nearest dangling OH group(s) (Cl···H′), and binding energies uncorrected ($-\Delta E_e^N$), corrected for basis set superposition error using the function counterpoise method but not for zero-point energies ($-\Delta E_e^B$), and corrected for both basis set superposition error and for zero-point energies ($-\Delta E_o^B$). [b] For methods using (nonlocal) plane waves, basis set superposition error is zero. [c] Reference 39. [d] Reference 41. Results are for globally minimized cyclic complexes HCl•$(H_2O)_n$ in which $n = 2$ and 3, respectively. [e] Results are for HCl on an isolated $(H_2O)_6$ cluster with a frozen, chair-shaped geometry. [f] Reference 42. [g] Reference 43. Their HF result is corrected for electron correlation by adding 9 kJ/mol determined using MP2.

cc-pVTZ and a cc-pVQZ basis set are 29 and 26 kJ/mol, respectively, while the binding energies corrected for basis set superposition error using the function counterpoise method[41,96,97] are 22 and 23 kJ/mol, respectively. The function counterpoise method only provides an upper limit to the true basis set superposition error. Accordingly, binding energies corrected for the *actual* basis set superposition error lie between 22−29 kJ/mol and 23−26 kJ/mol at the MP2 level of theory with cc-pVTZ and cc-pVQZ basis sets, respectively. (The range 23−26 kJ/mol is smaller because of the greater number of atomic basis functions in the cc-pVQZ basis set to describe the valence electrons participating in binding). We make the assumption that the midpoint of each range gives the best estimate of the binding energy. Therefore, 25.5 and 24.5 kJ/mol are our best estimates corrected for the *actual* basis set superposition error at the MP2 level of theory with a cc-pVTZ and a cc-pVQZ basis set, respectively. Extrapolating these results, a reasonable estimate of the MP2 binding energy in the infinite basis set limit is 24 kJ/mol.

Next, we provide an estimate of correlation effects not included in the MP2 method. Referring to Table 1, we estimate binding energies corrected for the *actual* basis set superposition error at the MP2 and QCISD(T) levels of theory with a 6-311++G(d,p) basis set to be 23.5 and 22 kJ/mol, respectively. This suggests a correction to the MP2 method for higher-order correlation effects of $22 - 23.5 = -1.5$ kJ/mol.

Adding our correction for higher-order correlation effects to our estimate of the MP2 binding energy in the infinite basis set limit, we obtain $24 - 1.5 = 22.5 = 23$ kJ/mol. This "basis set, correlation-corrected" binding energy is identical to the binding energy obtained for HCl•H_2O in the plane-wave calculation. We conclude that for the plane-wave method, the error resulting from the approximate form of the BLYP functional, the use of pseudopotentials, and a finite basis set all cancel each other. We can estimate the magnitude of the canceling errors: The binding energy corrected for the *actual* basis set superposition error using the BLYP functional with a (relatively large) cc-pVQZ basis set (and no pseudopotentials) is 23 kJ/mol, identical to the "basis set, correlation-corrected" result. We conclude that both the error associated with the use of the BLYP functional and with pseudopotentials/plane waves is zero for HCl•H_2O.

B. Cluster Model (4W1A). The geometry of HCl interacting with a water cluster representative of an adsorption site on the (0001) ice surface was determined and is reported in Table 2 and compared to results from Geiger et al.[39] and to other studies that used different cluster models.[41−43] Comparing our geometry for 4W1A to that for HCl•H_2O (Table 1), the HCl bond is slightly longer, while the hydrogen bond is 0.081 Å shorter and ∠OHCl is 15.4° smaller, consistent with results by Packer and Clary.[41] Distortion of both HCl and the water cluster in the complex is relatively minor, in agreement with Geiger et al.[39]

Examining the binding energies in Table 2,[98] our binding energy of 27 kJ/mol using plane waves and not corrected for zero-point energies is larger than that for HCl•H_2O, 23 kJ/mol (Table 1), which is consistent with the findings of Packer and Clary:[41] Their results of 32 and 30 kJ/mol for HCl•$(H_2O)_2$ and HCl•$(H_2O)_3$, respectively, are larger than their result for HCl•H_2O, 22 kJ/mol. Our binding energy of 27 kJ/mol is in excellent agreement with Geiger et al., 26 kJ/mol.[39] The values reported by Allouche et al.[42] and Bussolin et al.[43] for HCl

TABLE 3: Interaction of HCl with Slab Models[a]

slab model (method/basis set)	HCl (Å)	O···H (Å)	∠OHCl (deg)	Cl···H′ (Å)	μ_c (D)	μ_{fp} (D)	$-\Delta E_e^B$ (kJ/mol)	$-\Delta U_o^B$ (kJ/mol)	$-\Delta U_T^B$ (kJ/mol)	$-\Delta H_{200}^B$ (kJ/mol)
16W1A1Hf[b]	1.371	1.647	171.8	3.530	13.9	11.3	31	22	25	27
16W1A^{O2}1Hf[b]	1.357	1.742	171.0	3.692	14.0	11.0	30	21	24	26
16W1A^{O3}1Hf[b]	1.358	1.713	179.3	4.822	14.0	11.5	33	24	27	29
16W1A2Hf[b]	1.390	1.597	171.4	2.967, 3.358	1.9	4.8	36	27	30	32
32W1A2H[b]	1.389	1.595	171.6	2.957, 3.351	2.2	6.5	36	27	30	32
16W1A^{O2}2Hf[b]	1.369	1.654	171.5	3.522, 4.403	1.7	4.0	29	20	23	25
16W1A3Hf[b]	1.384	1.600	172.6	3.601, 3.732, 4.998	11.0	4.9	33	24	27	29
16W2A1Hf[b,c]	1.356	1.688	169.7	3.513	15.1	13.8	31	22	25	27
	1.337	1.856	173.2	4.892			21	12	15	17
16W2A2Hf[b,c]	1.368	1.678	169.6	2.911, 3.246	2.6	6.1	36	27	30	32
	1.353	1.717	171.8	3.820, 4.505			20	11	14	16
32W2A2H[b,c]	1.362	1.706	169.1	2.961, 3.301	3.2	8.6	36	27	30	32
	1.351	1.735	170.5	3.586, 4.471			20	11	14	16
other models[d]										
corr. HF/6-31G(d)[e]	1.29	1.90		3.63, 4.05			33	25		
classical[f]									19	
q.-classical[g]									25, 32, 33	
experiment[h]									$>35^{+3}_{-4}$, <25	
experiment[i]									$E_a^d = 26$	
experiment[j]									$E_a^d = 33(5)$	
experiment[k]										46

[a] Column headings are as follows: Optimized geometry, nearest dangling OH group(s) (Cl···H′), the total net dipole moment calculated assuming a constant dipole moment for each H_2O and HCl (μ_c) and also from first principles (μ_{fp}), binding energies corrected for basis set superposition error using the function counterpoise method but not for zero-point energies ($-\Delta E_e^B$) and for zero-point energies ($-\Delta E_o^B$) (emphasizing that no correction for basis set superposition error was done for the plane-wave calculations), binding energies at $T = 165$ K (unless noted otherwise) ($-\Delta U_T^B$), activation energies for desorption (E_a^d), and binding enthalpies at 200 K ($-\Delta H_{200}^B$). [b] For these models, density-functional theory with plane waves was used, and basis set superposition error is zero. [c] For these models, results for HCl adsorbed at O1 are given in the first row, while results for HCl adsorbed at O2 are given in the second row. [d] A model most similar to 16W1A2Hf was studied. [e] Reference 43. Their HF result is corrected for electron correlation by adding 9 kJ/mol determined using MP2, and the repulsion between HCl and its periodic image is subtracted out. [f] Reference 45, $T = 190$ K. [g] Reference 46. The three results are for HCl interacting with a defect-free (0001) face and faces with three and six water molecules removed, respectively, at 190 K. [h] Reference 31. Limits are for HCl on ice with low surface coverage and ice with high surface coverage of HCl, respectively. The uncertainty is indicated. [i] Reference 32. E_a^d was measured at 100−126 K. [j] Reference 33. E_a^d was measured at 140 K; the uncertainty is given in units of the last digit. [k] Reference 34.

adsorbed on a $(H_2O)_6$ cluster with a frozen, chair-shaped geometry are 11−13 kJ/mol larger, likely due to the formation of two weak hydrogen bonds between nearby dangling OH groups and chlorine in their model. The lengths of these hydrogen bonds are indicated in Table 2.

Making an argument similar to that in section IV A and referring to results in Table 2 obtained by Geiger et al.,[39] we estimate that the HCl binding energy for 4W1A corrected for the *actual* basis set superposition error at the MP2 level of theory with a 6-311++G(d,p) basis set is 30 kJ/mol. Interestingly, if we apply our correction for higher-order correlation effects obtained for HCl•H_2O of −1.5 kJ/mol, a binding energy only 1.5 kJ/mol larger than the plane-wave result is obtained.

According to our results in Table 2 using the BLYP functional with a 6-311++G(d,p) basis set, the zero-point correction is −9 kJ/mol. Our correction is close to −8 kJ/mol that was determined by Bussolin et al.[43] and to −11 and −12 kJ/mol that were determined by Packer and Clary[41] for HCl•$(H_2O)_2$ and HCl•$(H_2O)_3$, respectively. Although not shown in Table 2, binding energies $-\Delta U_T^B$ and enthalpies $-\Delta H_T^B$ at various temperatures T were also calculated. This was done using a thermal correction to the energy, $-\Delta U_{trans}(T) - \Delta U_{rot}(T) - \Delta U_{vib}(T)$, and an additional RT to obtain the enthalpy.[99,100] Results for 4W1A using the BLYP functional with a 6-311++G(d,p) basis set, which to within 1 kJ/mol are temperature independent from 165 to 200 K, are $-\Delta U_{200}^B = 24$ kJ/mol, and $-\Delta H_{200}^B = 26$ kJ/mol.

C. Infinite Surface Models. Following optimization of the ice slab models without HCl adsorbates, the geometry of the surface bilayer was found to be similar to that of optimized bulk ice I*h* described in an earlier paper.[13] This indicates that, at least at 0 K, surface reconstruction is minor. The change in distance between neighboring oxygen atoms was typically at most several hundredths of one Ångstrom. In all cases, the symmetric, hexagonal arrangement of molecules was preserved in the first (surface) bilayer.

Following optimization with HCl adsorbates using plane waves, a change of the Mulliken population[82,101−103] from −0.50 to −0.43 on the binding oxygen atom was typically observed, as was a change from 0.23 to 0.18 on the hydrogen atom and −0.08 to −0.19 on the chlorine atom of HCl. In terms of a Lewis-base argument, the oxygen atom of water partially donates a lone pair of electrons to HCl to form a hydrogen bond, and chlorine subsequently withdraws electrons from hydrogen. The changes for our slab models were similar to those for 4W1A, −0.50 to −0.45, 0.23 to 0.18, and −0.08 to −0.17, respectively. The charges on other atoms were essentially unchanged, consistent with a study of aqueous HCl dissociation to form a contact ion pair, the respective changes in that study being −0.975 to −0.593, 0.298 to 0.327, and −0.417 to −0.846.[104]

Calculated geometries for HCl interacting with five different slab models are shown in Table 3.[105] In our slab models, a single HCl molecule is almost always held more tightly than in 4W1A: The HCl bond is longer, the hydrogen bond lengths are typically shorter, and the ∠OHCl angles are greater. This trend is also observed in the study of Bussolin et al.[43] Also, the first bilayer of the slab is distorted upon adsorption; a change of ±0.1 Å between the adsorption site and adjacent oxygen atoms was typical.

Results for the binding energy of HCl are also given in Table 3.[106] Our $-\Delta U_T^B$ result for 16W1A2Hf agrees to within 3 kJ/

TABLE 4: Calculated Dipole−Dipole Interaction Energy, in kJ/mol, of HCl with the Entire Slab, with Only the Water Molecule Directly Involved in Binding, with the Binding H_2O and Its Nearest Neighbors, and with Each Layer

model	μ_c (D)	entire slab (kJ/mol)	binding H_2O (kJ/mol)	binding and neighboring H_2Os (kJ/mol)	layer 1 (kJ/mol)	layer 2 (kJ/mol)	layer 3 (kJ/mol)	layer 4 (kJ/mol)
16W1A1Hf	13.9	18.9	12.8	18.5	12.6	4.5	1.2	0.6
16W1A^{O2}1Hf	14.0	14.6	10.1	14.4	10.2	3.0	0.8	0.6
16W1A^{O3}1Hf	14.0	17.3	14.9	18.3	13.1	1.5	1.2	1.5
16W1A2Hf	1.9	20.1	11.7	17.1	12.3	6.7	0.5	0.6
16W1A^{O2}2Hf	1.7	18.9	13.0	19.0	13.6	5.1	0.0	0.2
16W1A3Hf	11.0	18.5	12.2	18.4	14.6	6.5	−2.1	−0.5

mol with that of Bussolin et al. using a nearly identical slab model but a different method,[43] despite the fact their hydrogen bond is substantially longer by 0.30 Å and that the distance between chlorine and the dangling OH groups is greater in their model, 3.63 and 4.05 Å vs 2.967 and 3.358 Å calculated here. However, HCl is less perturbed in their study, with only a 0.01 Å difference between the HCl bond length in the slab and the cluster vs 0.036 Å in this study. We also compare our $-\Delta U_T^B$ result of 30 kJ/mol for 16W1A2Hf with those obtained by Clary and Wang.[46] In their quantum-classical molecular dynamics study at 190 K of HCl interacting with a slab model consisting of 12 layers and 30 molecules per layer, the HCl bond length and distance of the center-of-mass from the surface were treated quantum mechanically but all other degrees of freedom were treated classically. Their $-\Delta U_T^B$ result for HCl interacting with a defect-free (0001) surface is 25 kJ/mol, larger than their purely classical result[45] of 19 kJ/mol and smaller than our $-\Delta U_T^B$ result of 30 kJ/mol. Their results for two slabs with defects are 32 and 33 kJ/mol, respectively.

An important conclusion from Table 3 is that our results for a slab with 32 water molecules are essentially identical to those for the slab with 16 water molecules with two dangling OH groups. This demonstrates that underlying layers do not affect surface adsorption for either one-molecule coverage, which is consistent with the results of others,[43] or for two-molecule coverage. This also demonstrates that the binding of HCl is unaffected by fixing the second bilayer. We believe these conclusions apply to slab models with one and three dangling OH groups as well, because the geometry changes for *all* models take place almost entirely at the adsorption site.

Our results in Table 3 also show that the average binding energy per site decreases by 5 kJ/mol, given a constant number of dangling OH groups, as coverage increases from one to two HCl molecules. This is likely due to the greater distortion of the first bilayer as well as the weak (few kJ/mol) dipolar repulsion between HCl adsorbates separated by 4−5 Å.

V. Further Discussion of Infinite-Surface-Model Results

To address the potential problem of overbinding of HCl, a dipolar molecule, on slab models with a large net dipole moment, and furthermore to understand better the mechanism of binding, the dipole−dipole interaction energy of HCl interacting with each water molecule in the slab was calculated directly.[107] As in section II, a dipole moment of 3.09 D for each water molecule and 1.11 D for HCl was assumed. The interaction of HCl with the periodic images of the water molecules was included. Our results are shown in Table 4. We conclude that despite the varying net dipole moments in the individual slabs, the HCl binding energy varies by only 5 kJ/mol and independently of net dipole moment. The lack of dependence is due to the inverse cubic dependence of interaction energy with increasing separation of the center-of-charges.[107] The water molecule interacting directly with HCl contributes by far the most to binding (60−90%). The dipolar interaction of HCl with the entire slab is always given to within 15% (and usually to within a few percent) by the interaction of HCl with the water molecule directly involved in binding and the three neighboring water molecules in the second layer to which that water molecule is hydrogen bonded.

A l^{-3} dependence of binding energy on hydrogen bond length l for three molecules with gas-phase dipole moments of 1.3 D (HOCl), 1.08 D (HCl), and 0 D (Cl_2) adsorbed on 4W was recently reported, and it was concluded dipolar coupling was largely responsible for binding.[39] For our slab models, comparing the binding energies in Tables 3 and 4 indicates that dipolar coupling is largely, though not entirely, responsible for binding. This conclusion is supported by plotting binding energy per site vs l using the plane-wave results from Tables 1−3, and noting that the best fit of the form cl^{-d}, where c and d are variables, is proportional to $l^{-3.11\pm0.91}$ ($R^2 = 0.49$). It is worth mentioning that hydrogen bonding (of hydrogen in HCl to oxygen in the water molecule) also contributes significantly to the binding energy. The contribution from layers three and four in Table 4 implies the contribution from hypothetical layers five and six would be small, further evidence that four layers are sufficient for modeling the interaction.

The effect of varying OH groups on binding is also significant. The binding energy of HCl at O1 vs O2 in our model with two dangling OH groups (16W1A2Hf vs 16W1A^{O2}2Hf) is larger by 7 kJ/mol. This difference is due to the fact that HCl at O1 is in close proximity to two dangling OH groups (Figure 2), which interact favorably with chlorine. As indicated in Table 3, the nearest OH groups are 3.522 and 4.403 Å from chlorine vs 2.967 and 3.358 Å when HCl is adsorbed at O1. Not surprisingly, because of these interactions, HCl is stretched to a greater extent, and the surface is more distorted as neighboring water molecules rearrange to bind with the chlorine atom.

Although HCl binding at sites in close proximity to dangling OH groups is energetically more favorable, binding at sites where there are few or no OH groups to interact appreciably with HCl is quite possibly *more* representative of adsorption on Type II PSC particles. Crystalline ice is conjectured not to have a high surface density of dangling OH groups based on a comparison of the vibrational spectrum and surface properties of crystalline and amorphous ice.[108] The actual surface density of dangling OH groups on crystalline ice is, however, not known definitively. On liquid water, it is estimated using infrared-visible sum-frequency generation to be more than 20%.[109]

Assuming a molecular HCl surface coverage corresponding to one molecule per simulation cell (1.4×10^{14} molecule/cm^2), from Table 3 we estimate a range of binding energies of 23−30 kJ/mol and binding enthalpies of 25−32 kJ/mol at 185 K. However, the lower end of the range may be more likely and adsorption may best be modeled on 16W1Hf or at O2 in 16W2Hf due to the conjectured low surface density of dangling

OH groups on crystalline ice. For a surface coverage corresponding to 2.8×10^{14} molecule/cm^2, the binding energy and enthalpy per site are 14−30 and 16−32 kJ/mol, respectively. The average binding energy and enthalpy per site are 20−22 and 22−24 kJ/mol, respectively, where again the lower end of the range may be more likely.

For a low (submonolayer) coverage corresponding to one molecule per simulation cell (1.4×10^{14} molecule/cm^2), from the preceding discussion we conclude reasonable, accurate values for the binding energy and enthalpy of HCl on Type II PSCs are 23 and 25 kJ/mol, respectively. For a higher (monolayer) coverage corresponding to two molecules per simulation cell (2.8×10^{14} molecule/cm^2), reasonable values for the average binding energy and enthalpy are 20 and 22 kJ/mol, respectively. These estimates, independent of temperature between 165 and 200 K (and only slightly less at lower temperatures), agree with some of the experimental data, which exhibits a wide range, given in Table 3. Andersson et al. also report a decrease, albeit larger, of binding energy with increasing HCl coverage in their molecular beam study.[31] Their absolute binding energies may be larger than ours due to the high temperature of the measurements, which may mean processes more complicated than simple adsorption are occurring at the ice surface. Agreeing well with our estimated binding energy of 23 kJ/mol, Isakson and Sitz estimate the activation energy of desorption to be 26 kJ/mol for low HCl coverage.[32] Their result was obtained on crystalline ice (at least) several thousand Ångstroms thick. Our slab models, with the bottom bilayer fixed, may *more* accurately depict this type of surface rather than the ultrathin (5−20 monolayers thick) ice films studied by Graham and Roberts.[33] According to these authors, their films are likely rich in defects, and thus may have a higher density of dangling OH groups, which would explain why their activation energy of desorption of 33 kJ/mol is larger. Preliminary experimental results from our group indicate a binding enthalpy of 25−30 kJ/mol for low HCl coverage, 16−21 kJ/mol smaller than Elliott et al.[34] but which agrees well with our estimate given above of 25 kJ/mol.

Besides the fact the surface density of dangling OH groups and the surface coverage of HCl on Type II PSCs are unknown, there may be other sources of error. Although our binding energy for HCl•H_2O agrees to within 1 kJ/mol with a high-level theoretical estimate, implying cancellation of errors associated with use of the BLYP functional and psedopotentials/plane waves, there is no guarantee the same is true for our slab models. Also, our zero-point and thermal corrections are harmonic approximations.

VI. Atmospheric Relevance and Future Work

Correlated with adsorption, a slight elongation of HCl (by up to 0.086 Å, 7%) occurs at all sites, but dissociation is not observed, even though our homolytic dissociation energy for HCl is underestimated by 25 kJ/mol (6%). This indicates that there is a barrier to dissociation of HCl of unknown magnitude but does not indicate whether molecular or ionized HCl is more stable at 185 K. This barrier may be as large as 33.9−6.3 = 28 kJ/mol based on a rough estimate for HCl atop an ice surface (versus 0.4 kJ/mol for HCl incorporated into the first bilayer of the ice lattice).[110] Preliminary theoretical results from our group indicate that under certain circumstances it may be significantly less. With a better understanding of the processes that HCl undergoes initially during adsorption, we are interested in elucidating the subsequent fate of HCl at the ice surface to understand better chlorine activation, i.e., Rx. (1). We are investigating the possibility of ionization of HCl following adsorption using ab initio molecular dynamics[13] in conjunction with experiments under typical polar stratospheric conditions.

VII. Conclusions

In this work, both cluster and extended surface models of the hexagonal ice basal (0001) face for modeling the interaction of HCl on Type II PSC particles were described, and results for the molecular adsorption of HCl on each were compared in section IV. Our molecular HCl binding energy at 0 K corrected for zero-point error is 27 kJ/mol for HCl adsorbed in close proximity to two dangling OH groups on a periodic slab model. This value is very similar to 25 kJ/mol from Bussolin et al. using a different method.[43]

As discussed in section V, our best estimate of the binding energy and enthalpy of molecular HCl on hexagonal ice I*h* crystals at 165−200 K (assuming molecular HCl does in fact exist) are 23 and 25 kJ/mol, respectively, for low (single-molecule) HCl coverage, decreasing to 20 and 22 kJ/mol, respectively, as the coverage of HCl increases. Our estimates would be a few kJ/mol smaller at lower temperatures, decreasing to 20 kJ/mol (low coverage) and 17 kJ/mol (high coverage) at 0 K. These estimates are based on a low surface density of dangling (non-hydrogen-bonding) OH groups.

Our results also indicate that there is a barrier of unknown magnitude to the ionization of HCl upon adsorption. We are investigating the possible ionization of HCl following adsorption, a question of great atmospheric importance, at stratospherically relevant temperatures using the results of this work.

Acknowledgment. This work was partially supported by the NASA Upper Atmospheric Research Program under Grant No. NAG5-8887. Y.A.M. acknowledges partial support from the MIT Center for Global Change Sciences. F.M.G. acknowledges support from the NOAA Postdoctoral Program in Climate and Global Change, administered by the University Corporation for Atmospheric Research. This work was also partially supported by the National Computational Science Alliance under a Boston University MARINER/Alliance startup allocation (Project No. 60390) and under Proposal No. CTS990016N and utilized the Boston University SGI/CRAY Origin2000 and the NCSA SGI/CRAY Origin2000, respectively.

Supporting Information Available: Our optimized structures in Tables 1, 2, and 3; a computer program to find ice slab models with a net dipole moment as small as possible; and a program to calculate the net dipole moment with and without HCl adsorbates. This information is available free of charge via the Internet at http://pubs.acs.org.

References and Notes

(1) Molina, M. J. *Angew. Chem. Int. Ed. Engl.* **1996**, *35*, 1778.
(2) Chang, H.-Y. A.; Koop, T.; Molina, L. T.; Molina, M. J. *J. Phys. Chem. A* **1999**, *103*, 2673.
(3) Tabazadeh, A.; Toon, O. B.; Jensen, E. J. *Geophys. Res. Lett.* **1997**, *24*, 2007.
(4) Turco, R. P.; Toon, O. B.; Hamill, P. *J. Geophys. Res.* **1989**, *94D*, 16493.
(5) List, R. J. *Smithsonian Meteorological Tables*, 6th ed.; Smithsonian Institution: Washington, DC, 1951.
(6) Seinfeld, J. H.; Pandis, S. N. *Atmospheric Chemistry and Physics: From Air Pollution to Climate Change*; Wiley: New York, 1998.
(7) Lee, S.-H.; Leard, D. C.; Zhang, R.; Molina, L. T.; Molina, M. J. *Chem. Phys. Lett.* **1999**, *315*, 7.
(8) Horn, A. B.; Sodeau, J. R.; Roddis, T. B.; Williams, N. A. *J. Phys. Chem. A* **1998**, *102*, 6107.
(9) Oppliger, R.; Allanic, A.; Rossi, M. J. *J. Phys. Chem. A* **1997**, *101*, 1903.

(10) Sander, S. P.; Friedl, R. R.; DeMore, W. B.; Golden, D. M.; Kurylo, M. J.; Hampson, R. F.; Huie, R. E.; Moortgat, G. K.; Ravishankara, A. R.; Kolb, C. E.; Molina, M. J. *Chemical Kinetics and Photochemical Data for Use in Stratospheric Modeling, Supplement to Evaluation 12: Update of Key Reactions*; Jet Propulsion Laboratory: Pasadena, CA, 2000.

(11) Molina, L. T.; Molina, M. J.; Stachnik, R. A.; Tom, R. D. *J. Phys. Chem.* **1985**, *89*, 3779.

(12) Petrenko, V. F.; Whitworth, R. W. *Physics of Ice*; Oxford University Press: New York, 1999.

(13) Mantz, Y. A.; Geiger, F. M.; Molina, L. T.; Molina, M. J.; Trout, B. L. *J. Chem. Phys.* **2000**, *113*, 10733.

(14) Molina, M. J. The Probable Role of Stratospheric "Ice" Clouds: Heterogeneous Chemistry of the "Ozone Hole". In *The Chemistry of the Atmosphere: Its Impact on Global Change*; Calvert, J. G., Ed.; Blackwell Scientific Publications: Oxford, 1994; p 27.

(15) Gertner, B. J.; Hynes, J. T. *Science* **1996**, *271*, 1563.

(16) Gertner, B. J.; Hynes, J. T. *Faraday Discuss.* **1998**, *110*, 301.

(17) George, S. M.; Livingston, F. E. *Surf. Rev. Lett.* **1997**, *4*, 771.

(18) Bianco, R.; Hynes, J. T. *J. Phys. Chem. A* **1999**, *103*, 3797.

(19) McNamara, J. P.; Tresadern, G.; Hillier, I. H. *J. Phys. Chem. A* **2000**, *104*, 4030.

(20) Mebel, A. M.; Morokuma, K. *J. Phys. Chem.* **1996**, *100*, 2985.

(21) Kroes, G.-J. *Comments At. Mol. Phys.* **1999**, *34*, 259.

(22) Leu, M.-T.; Keyser, L. F.; Timonen, R. S. *J. Phys. Chem. B* **1997**, *101*, 6259.

(23) Foster, K. L.; Tolbert, M. A.; George, S. M. *J. Phys. Chem. A* **1997**, *101*, 4979.

(24) Pursell, C. J.; Zaidi, M.; Thompson, A.; Fraser-Gaston, C.; Vela, E. *J. Phys. Chem. A* **2000**, *104*, 552.

(25) Delzeit, L.; Powell, K.; Uras, N.; Devlin, J. P. *J. Phys. Chem. B* **1997**, *101*, 2327.

(26) Banham, S. F.; Sodeau, J. R.; Horn, A. B.; McCoustra, M. R. S.; Chesters, M. A. *J. Vac. Sci. Technol. A* **1996**, *14*, 1620.

(27) Donsig, H. A.; Vickerman, J. C. *J. Chem. Soc., Faraday Trans.* **1997**, *93*, 2755.

(28) Abbatt, J. P. D.; Beyer, K. D.; Fucaloro, A. F.; McMahon, J. R.; Wooldridge, P. J.; Zhang, R.; Molina, M. J. *J. Geophys. Res.* **1992**, *97D*, 15819.

(29) Hanson, D. R.; Mauersberger, K. *J. Phys. Chem.* **1990**, *94*, 4700.

(30) Sadtchenko, V.; Giese, C. F.; Gentry, W. R. *J. Phys. Chem. B* **2000**, *104*, 9421.

(31) Andersson, P. U.; Någård, M. B.; Pettersson, J. B. C. *J. Phys. Chem. B* **2000**, *104*, 1596.

(32) Isakson, M. J.; Sitz, G. O. *J. Phys. Chem. A* **1999**, *103*, 2044.

(33) Graham, J. D.; Roberts, J. T. *J. Phys. Chem.* **1994**, *98*, 5974.

(34) Elliott, S.; Turco, R. P.; Toon, O. B.; Hamill, P. *J. Atmos. Chem.* **1991**, *13*, 211.

(35) Uras, N.; Rahman, M.; Devlin, J. P. *J. Phys. Chem. B* **1998**, *102*, 9375.

(36) Atkins, P. W. *Physical Chemistry*, 5th ed.; W. H. Freeman & Co.: New York, 1994.

(37) Rossini, F. D. *J. Res. Nat. Bur. Stand.* **1932**, *9*, 679.

(38) Bacelo, D. E.; Binning, R. C., Jr.; Ishikawa, Y. *J. Phys. Chem. A* **1999**, *103*, 4631.

(39) Geiger, F. M.; Hicks, J. M.; de Dios, A. C. *J. Phys. Chem. A* **1998**, *102*, 1514.

(40) Re, S.; Osamura, Y.; Suzuki, Y.; Schaefer, H. F., III. *J. Chem. Phys.* **1998**, *109*, 973.

(41) Packer, M. J.; Clary, D. C. *J. Phys. Chem.* **1995**, *99*, 14323.

(42) Allouche, A.; Couturier-Tamburelli, I.; Chiavassa, T. *J. Phys. Chem. B* **2000**, *104*, 1497.

(43) Bussolin, G.; Casassa, S.; Pisani, C.; Ugliengo, P. *J. Chem. Phys.* **1998**, *108*, 9516.

(44) Kroes, G.-J.; Clary, D. C. *J. Phys. Chem.* **1992**, *96*, 7079.

(45) Kroes, G.-J.; Clary, D. C. *Geophys. Res. Lett.* **1992**, *19*, 1355.

(46) Clary, D. C.; Wang, L. *J. Chem. Soc., Faraday Trans.* **1997**, *93*, 2763.

(47) Jorgensen, W. L.; Chandrasekhar, J.; Madura, J. D.; Impey, R. W.; Klein, M. L. *J. Chem. Phys.* **1983**, *79*, 926.

(48) Estrin, D. A.; Kohanoff, J.; Laria, D. H.; Weht, R. O. *Chem. Phys. Lett.* **1997**, *280*, 280.

(49) Planas, M.; Lee, C.; Novoa, J. J. *J. Phys. Chem.* **1996**, *100*, 16495.

(50) Casassa, S. *Chem. Phys. Lett.* **2000**, *321*, 1.

(51) Robertson, S. H.; Clary, D. C. *Faraday Discuss.* **1995**, *100*, 309.

(52) Svanberg, M.; Pettersson, J. B. C.; Bolton, K. *J. Phys. Chem. A* **2000**, *104*, 5787.

(53) For ice I*h*, there are six symmetry-related planes parallel to the hexagonal axis *c* (or *z*) passing through origin *o*. These so-called prism faces (and, for consistency, the orthogonal basal faces) are named using Miller−Bravais indices in order not to obscure the symmetry relations: The plane (*hkil*) makes axial intercepts in the ratio *a*/*h*:*a*/*k*:*a*/*i*:*c*/*l*, where indices *h*, *k*, *i*, and *l* refer, respectively, to redundant axes *ox*, *oy*, and *ou* separated by 120° and *oz*. From Megaw (ref 58).

(54) Sprik, M.; Hutter, J.; Parrinello, M. *J. Chem. Phys.* **1996**, *105*, 1142.

(55) Bernal, J. D.; Fowler, R. H. *J. Chem. Phys.* **1933**, *1*, 515.

(56) Materer, N.; Starke, U.; Barbieri, A.; Van Hove, M. A.; Somorjai, G. A.; Kroes, G.-J.; Minot, C. *Surf. Sci.* **1997**, *381*, 190.

(57) Fletcher, N. H. *The Chemical Physics of Ice*; Cambridge University Press: New York, 1970.

(58) Megaw, H. D. *Crystal Structures*; TechBooks: Fairfax, VA, 1973 (first year of publication).

(59) Hayward, J. A.; Reimers, J. R. *J. Chem. Phys.* **1997**, *106*, 1518.

(60) Rahman, A.; Stillinger, F. H. *J. Chem. Phys.* **1972**, *57*, 4009.

(61) Batista, E. R.; Xantheas, S. S.; Jónsson, H. *J. Chem. Phys.* **1998**, *109*, 4546.

(62) Batista, E. R.; Xantheas, S. S.; Jónsson, H. *J. Chem. Phys.* **1999**, *111*, 6011.

(63) Vanderbilt, D.; King-Smith, R. D. *Phys. Rev. B* **1993**, *48*, 4442.

(64) King-Smith, R. D.; Vanderbilt, D. *Phys. Rev. B* **1993**, *47*, 1651.

(65) Kohn, W. *Rev. Mod. Phys.* **1999**, *71*, 1253.

(66) Parr, R. G.; Yang, W. *Density-Functional Theory of Atoms and Molecules*; Oxford University Press: New York, 1989.

(67) Parrinello, M. *Solid State Commun.* **1997**, *102*, 107.

(68) Galli, G.; Pasquarello, A. First Principles Molecular Dynamics. In *Computer Simulations in Chemical Physics*; Allen, M. P., Tildesley, D. J., Eds.; Kluwer Academic Publishers: Dordrecht, 1993; Vol. 397; p 261.

(69) Payne, M. C.; Teter, M. P.; Allan, D. C.; Arias, T. A.; Joannopoulos, J. D. *Rev. Mod. Phys.* **1992**, *64*, 1045.

(70) Becke, A. D. *Phys. Rev. A* **1988**, *38*, 3098.

(71) Lee, C.; Yang, W.; Parr, R. G. *Phys. Rev. B* **1988**, *37*, 785.

(72) Troullier, N.; Martins, J. L. *Phys. Rev. B* **1991**, *43*, 1993.

(73) Cohen, M. L. *Phys. Today* **1979**, *32*, 40 (July issue).

(74) Hutter, J.; Alavi, A.; Deutsch, T.; Bernasconi, M.; Goedecker, St.; Marx, D.; Tuckerman, M.; Parrinello, M. *CPMD*; Max-Planck Institut für Festkörperforschung and IBM Zurich Research Laboratory, 1995−99.

(75) Fischer, T. H.; Almlöf, J. *J. Phys. Chem.* **1992**, *96*, 9768.

(76) Császár, P.; Pulay, P. *J. Mol. Struct.* **1984**, *114*, 31.

(77) Kirkpatrick, S.; Gelatt, C. D., Jr.; Vecchi, M. P. *Science* **1983**, *220*, 671.

(78) Huber, K. P.; Herzberg, G. *Molecular Spectra and Molecular Structure IV. Constants of Diatomic Molecules*; Van Nostrand: New York, 1979.

(79) Benedict, W. S.; Gailer, N.; Plyler, E. K. *J. Chem. Phys.* **1956**, *24*, 1139.

(80) Frisch, M. J.; Trucks, G. W.; Schlegel, H. B.; Gill, P. M. W.; Johnson, B. G.; Robb, M. A.; Cheeseman, J. R.; Keith, T. A.; Petersson, G. A.; Montgomery, J. A.; Raghavachari, K.; Al-Laham, M. A.; Zakrzewski, V. G.; Ortiz, J. V.; Foresman, J. B.; Cioslowski, J.; Stefanov, B. B.; Nanayakkara, A.; Challacombe, M.; Peng, C. Y.; Ayala, P. Y.; Chen, W.; Wong, M. W.; Andres, J. L.; Replogle, E. S.; Gomperts, R.; Martin, R. L.; Fox, D. J.; Binkley, J. S.; Defrees, D. J.; Baker, J.; Stewart, J. P.; Head-Gordon, M.; Gonzalez, C.; Pople. J. A. *Gaussian 94*, Revision E.3; Gaussian, Inc.: Pittsburgh, PA, 1995.

(81) Møller, C.; Plesset, M. S. *Phys. Rev.* **1934**, *46*, 618.

(82) Szabo, A.; Ostlund, N. S. *Modern Quantum Chemistry: Introduction to Advanced Electronic Structure Theory*, 2nd ed.; Dover: New York, 1989.

(83) For H and O, the 6-311G basis and polarization functions of Krishnan et al. (ref 84). For Cl, a (12s9p)/[631111, 52111] "negative-ion/Cl$^-$" basis (ref 85) and polarization functions of Francl et al. (ref 86). Diffuse functions from Frisch et al. (ref 87), who cites Clark et al. (ref 88).

(84) Krishnan, R.; Binkley, J. S.; Seeger, R.; Pople, J. A. *J. Chem. Phys.* **1980**, *72*, 650.

(85) McLean, A. D.; Chandler, G. S. *J. Chem. Phys.* **1980**, *72*, 5639.

(86) Francl, M. M.; Pietro, W. J.; Hehre, W. J.; Binkley, J. S.; Gordon, M. S.; DeFrees, D. J.; Pople, J. A. *J. Chem. Phys.* **1982**, *77*, 3654.

(87) Frisch, M. J.; Pople, J. A.; Binkley, J. S. *J. Chem. Phys.* **1984**, *80*, 3265.

(88) Clark, T.; Chandrasekhar, J.; Spitznagel, G. W.; Schleyer, P. v. R. *J. Comput. Chem.* **1983**, *4*, 294.

(89) Obtained by Gaussian, Inc., from the Extensible Computational Chemistry Environment Basis Set Database, as developed and distributed by the Molecular Science Computing Facility, Environmental and Molecular Sciences Laboratory which is part of the Pacific Northwest Laboratory, P.O. Box 999, Richland, WA 99352, and funded by the U.S. Department of Energy. The Pacific Northwest Laboratory is a multi-program laboratory operated by Battelle Memorial Institute for the U.S. Department of Energy under contract DE-AC06-76RLO 1830. For primitive exponents (1st column) and coefficients (2nd−*n*th columns), select CODE: SUPERMOLECULE or Dalton at http://www.emsl.pnl.gov:2080/forms/basisform.html. Also see Dunning (ref 90) and Woon and Dunning (ref 91). Contact David Feller or Karen Schuchardt for further information.

(90) Dunning, T. H., Jr. *J. Chem. Phys.* **1989**, *90*, 1007.

(91) Woon, D. E.; Dunning, T. H., Jr. *J. Chem. Phys.* **1993**, *98*, 1358.

(92) Pople, J. A.; Head-Gordon, M.; Raghavachari, K. *J. Chem. Phys.* **1987**, *87*, 5968.

(93) Wong, M. W. *Chem. Phys. Lett.* **1996**, *256*, 391.
(94) Scott, A. P.; Radom, L. *J. Phys. Chem.* **1996**, *100*, 16502.
(95) Legon, A. C.; Willoughby, L. C. *Chem. Phys. Lett.* **1983**, *95*, 449.
(96) Uncorrected binding energies $-\Delta E_e^N$ were calculated, as well as $-\Delta E_e^B$ corrected for basis set superposition error *BSSE* (as indicated by a superscript B) but not for zero-point energies (as indicated by a subscript e) using $-\Delta E_e^B = -\Delta E_e^N + BSSE = D_e^{HCl\cdot H_2O} - D_e^{HCl} - D_e^{H_2O} + BSSE$, where $D_e = -E_e > 0$, and $BSSE = D_e^{HCl--}(\chi_{HCl}) - D_e^{HCl--}(\chi_{HCl}\chi_{H_2O}) + D_e^{H_2O}(\chi_{H_2O}) - D_e^{--H_2O}(\chi_{HCl}\chi_{H_2O})$. Here, $D_e^{HCl--}(\chi_{HCl}\chi_{H_2O})$ is the absolute energy of HCl in the full dimer basis $\chi_{HCl}\chi_{H_2O}$ and in the cluster geometry, $D_e^{HCl--}(\chi_{HCl})$ is the absolute energy of HCl with only its own basis set χ_{HCl} but again at the geometry it has within the cluster, and so on (ref 41, 97). For methods using localized basis sets, $BSSE < 0$, but $BSSE = 0$ using a plane-wave (nonlocalized) basis set, in principle for any value of the basis-set cutoff.
(97) Boys, S. F.; Bernardi, F. *Mol. Phys.* **1970**, *19*, 553.
(98) To calculate $-\Delta E_e^N$ and $-\Delta E_e^B$, the equations given in ref 96 were used after replacing H_2O with the cluster model. In addition, $-\Delta E_o^B$ corrected for both *BSSE* and for zero-point energies (as indicated by a subscript o) were calculated using $-\Delta E_o^B = -\Delta E_o^N + BSSE = D_o^{4W1A} - D_o^{HCl} - D_o^{4W} + BSSE$, where $D_o \approx D_e - {}^1/_2\omega_e$, and *BSSE* is defined as in ref 96.
(99) Binding energy $-\Delta U_T^B$ at temperature T was calculated using $-\Delta U_T^B = -\Delta E_o^B - \Delta U_{trans}(T) - \Delta U_{rot}(T) - \Delta U_{vib}(T) = -\Delta E_o^B + 5/2\,RT - \Delta U_{vib}(T)$, where in this equation $-\Delta U_{trans}(T) = U_{trans}^{HCl}(T) + U_{trans}^{4W}(T) - U_{trans}^{4W1A}(T) = {}^3/_2RT$, $-\Delta U_{rot}(T) = U_{rot}^{HCl}(T) + U_{rot}^{4W}(T) - U_{rot}^{4W1A}(T) = RT$, and $-\Delta U_{vib}(T) = U_{vib}^{HCl}(T) + U_{vib}^{4W}(T) - U_{vib}^{4W1A}(T) < 0$. The binding enthalpy $-\Delta H_T^B = -\Delta U_T^B + RT$.
(100) McQuarrie, D. A. *Statistical Mechanics*; HarperCollins: New York, 1976.
(101) To calculate Mulliken populations (ref 102), the wave functions calculated using plane waves are first projected onto atomic pseudo-wave functions. These are described by a minimal basis of Slater orbitals for the valence electrons, with exponents taken from the Clementi−Raimondi table (ref 103).
(102) Mulliken, R. S. *J. Chem. Phys.* **1955**, *23*, 1833.
(103) Clementi, E.; Raimondi, D. L. *J. Chem. Phys.* **1963**, *38*, 2686.
(104) Ando, K.; Hynes, J. T. *J. Phys. Chem. B* **1997**, *101*, 10464.
(105) Results for a slab with no dangling OH groups (16W*y*A0Hf, where $y = 1-4$), as well as for a slab with one dangling OH group (16W3A1Hf) that satisfied the ice rules were obtained. However, convergence was very slow, and sometimes HCl was dissociated in the "optimized" geometry. We believe HCl dissociation was a consequence of long-range dipole-dipole coupling between periodic images.
(106) For our plane-wave results, $BSSE = 0$, hence $-\Delta E_e^B = -\Delta E_e^N$. Our zero-point correction (−9 kJ/mol) and thermal contributions to the energy (3 kJ/mol) and enthalpy (5 kJ/mol) for 4W1A were used to estimate $-\Delta E_o^B = -\Delta E_e^B - 9$ kJ/mol, $-\Delta U_{165}^B = -\Delta E_o^B + 3$ kJ/mol, and $-\Delta H_{200}^B = -\Delta E_o^B + 5$ kJ/mol for the slab models.
(107) Maitland, G. C.; Rigby, M.; Smith, E. B.; Wakeham, W. A. *Intermolecular Forces: Their Origin and Determination*; Oxford University Press: New York, 1981.
(108) Schaff, J. E.; Roberts, J. T. *J. Phys. Chem.* **1994**, *98*, 6900.
(109) Du, Q.; Superfine, R.; Freysz, E.; Shen, Y. R. *Phys. Rev. Lett.* **1993**, *70*, 2313.
(110) Bianco, R.; Gertner, B. J.; Hynes, J. T. *Ber. Bunsenges. Phys. Chem.* **1998**, *102*, 518.